

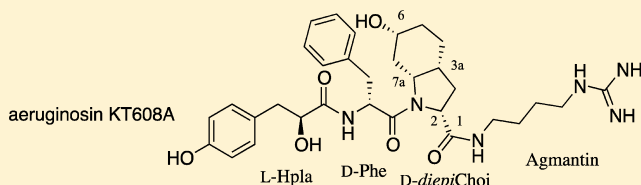
## Metabolites of *Microcystis aeruginosa* Bloom Material from Lake Kinneret, Israel

Marina Lifshits and Shmuel Carmeli\*

Raymond and Beverly Sackler School of Chemistry and Faculty of Exact Sciences, Tel-Aviv University, Ramat Aviv, Tel-Aviv 69978, Israel

### Supporting Information

**ABSTRACT:** Six new metabolites, micropeptin KT1042, microguanidine KT636, aeruginosins KT608A, KT608B, and KT650, and pseudoaeruginosin KT554, were isolated along with the known micropeptins SF909 and HM978, cyanopeptolin S, anabaenopeptin F, and the two isomers of planktocyclusin-S-oxide from a bloom material collected from Lake Kinneret, Israel, in March 2005. The structure elucidation and biological activity of the six new natural products isolated from this bloom material and the related aeruginosin GH553 are described.



Marine and freshwater bloom-forming genera of cyanobacteria are well known for the structural diversity of their secondary metabolites and for the high structural variation within each particular group of metabolites.<sup>1,2</sup> Freshwater toxic cyanobacteria are among the most studied genera of cyanobacteria due to their serious threat to human health.<sup>3</sup> More than 80 different members of the hepatotoxic microcystins, which are produced by water-bloom-forming genera of cyanobacteria, are known to date.<sup>4</sup> They are usually accompanied by the micropeptins, a group of serine protease inhibitors that includes more than 130 members,<sup>5</sup> the anabaenopeptins (38 isolated variants),<sup>6</sup> the aeruginosins (19 isolated variants),<sup>7</sup> the microginins (34 isolated variants),<sup>8</sup> the microviridins (15 isolated variants),<sup>9</sup> and many other compounds that are not grouped together. All of these compounds are peptidic in nature, but they usually contain certain structural elements that interfere with their hydrolysis by proteolytic enzymes, such as  $\beta$ -amino acids (aa's), long chain aa's, dehydro aa's, modified aa's, iso-linked aa's, *N*-methylated aa's, *D*-aa's, and other isomeric aa's. In certain cases *allo*-amino acids are incorporated into the backbone of these peptides. Most of the aeruginosins belong to one group that contains the proline-mimicking amino acid *L*-2-carboxy-6-hydroxyoctahydroindole (*L*-Choi),<sup>7</sup> while only one, aeruginosin EI461, contains the *L*-diepi-Choi.<sup>10,11</sup> As part of our ongoing research on the chemistry and chemical ecology of cyanobacterial blooms in water bodies, the biomass of bloom material (TAU strain IL-347) of *Microcystis aeruginosa* collected from Lake Kinneret, Israel, in March 2005 was chemically investigated. The extract of this bloom afforded some unusual isomeric compounds belonging to the micropeptins and aeruginosins. All of the isolated aeruginosins contain a new (2*R*,3*aR*,6*R*,7*aR*)-Choi (*D*-3*a*,7*a*-diepi-Choi) moiety. The isolation and structure elucidation of the new secondary metabolites isolated from this cyanobacterial bloom biomass and the related aeruginosin GH553,<sup>12</sup> their biological activities, and the biogenesis of this new group of aeruginosins are discussed below.

### RESULTS AND DISCUSSION

The bloom material was separated in the laboratory to an aqueous solution and cells by aggregation with alum. The cells were immediately frozen after separation and freeze-dried. The aqueous solution (12 L) was passed through an Amberlite XAD-2 column and extracted thereafter with MeOH. The MeOH extract, which inhibited trypsin and chymotrypsin, was flash chromatographed on a reversed-phase C<sub>18</sub> column. The fractions that exhibited protease inhibitory activity were further separated by gel filtration on a Sephadex LH-20 column and reversed-phase HPLC columns to afford six pure natural products: micropeptins KT1042 (1), HM978,<sup>13</sup> and SF909<sup>14</sup> and aeruginosins KT608A (3), KT608B (4), and KT650 (5). The freeze-dried cyanobacterium biomass was extracted with 70% MeOH in H<sub>2</sub>O. The cell extract was separated in the same way as the aqueous extract to afford micropeptins KT1042 (1), HM978,<sup>13</sup> and SF909,<sup>14</sup> cyanopeptolin S,<sup>15</sup> microguanidine KT636 (2), aeruginosins KT608A (3), KT608B (4), and KT650 (5), pseudoaeruginosin KT554 (6), anabaenopeptin F,<sup>16</sup> and the two *S*-oxide isomers of planktocyclusin-*S*-oxide (see Figure S50 in the Supporting Information).<sup>17,18</sup>

Micropeptin KT1042 (1) was isolated as a colorless, glassy material. It presented a sodiated MALDI TOF quasimolecular ion at  $m/z$  1065.4971, in agreement with the molecular formula C<sub>53</sub>H<sub>70</sub>N<sub>8</sub>NaO<sub>14</sub>. The NMR spectra of 1 in DMSO-*d*<sub>6</sub> (Table 1) revealed its peptidic nature and that it belongs to the micropeptins, i.e., nine carbonyl carbons in the <sup>13</sup>C NMR spectrum, five secondary amide doublet and two primary amide singlet protons, two hydroxy protons resonating at  $\delta_H$  6.04 (brd) and 5.51 (brs), and an NMe group  $\delta_H$  2.56 (s), in the <sup>1</sup>H NMR spectrum. Taking into account the characteristic NMe-aromatic amino acid and the *N,N*-disubstituted-amino acid of the micropeptins, the five amide doublet protons revealed that this micropeptin was composed of seven amino acids. The existence

Received: November 16, 2011

Published: January 26, 2012

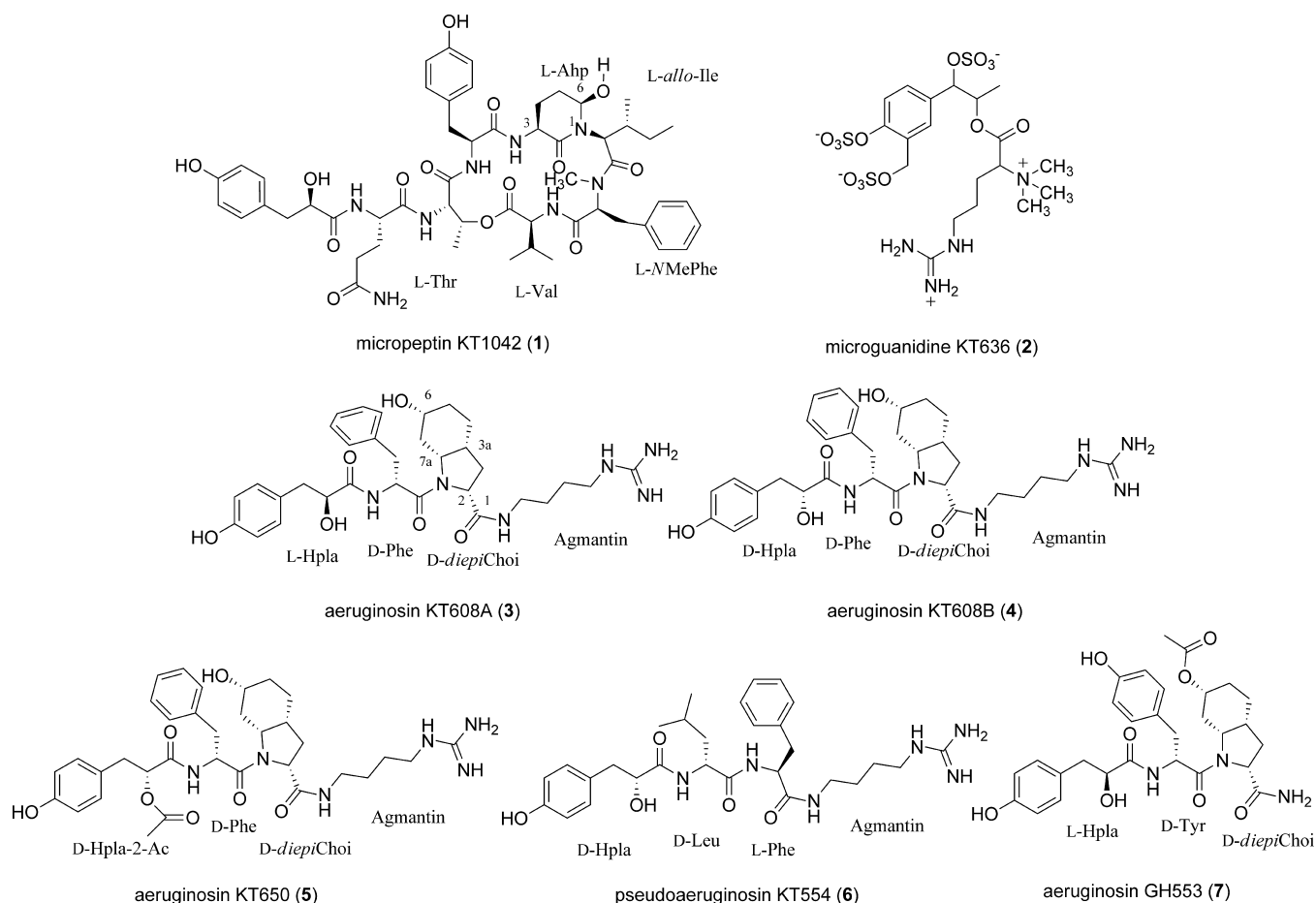
Table 1. NMR Data of Micropeptin KT1042 (1) in DMSO-*d*<sub>6</sub><sup>a</sup>

position	$\delta_C$ , mult. <sup>b</sup>	$\delta_H$ , mult., J (Hz)	HMBCcor- relations <sup>c</sup>	NOE correlations <sup>d</sup>	position	$\delta_C$ , mult. <sup>b</sup>	$\delta_H$ , mult., J (Hz)	HMBCcor- relations <sup>c</sup>	NOE correlations <sup>d</sup>
Val 1	172.4, C				6	74.2, CH	4.90, brs	Ahp-4	Ahp-5,6-OH, Ile-3
2	56.4, CH	4.70, dd (9.6, 5.2)	Val-1,3,4,5, NMePhe-1	Val-3,4,5,NH	6-OH		6.04, brs		Ahp-4b,6, Val-5,NH
3	30.9, CH	2.05, m	Val-4,5	Val-2,4,5,NH	NH		7.35, d (9.0)	Ahp-3, Tyr-1	Ahp-3,4b, Thr-3, Tyr-NH
4	19.4, CH <sub>3</sub>	0.83, d (6.7)	Val-2,3	Val-2,3,NH, NMe- Phe-NMe	Tyr 1	170.2, C			
5	17.8, CH <sub>3</sub>	0.72, d (6.7)	Val-2,3	Val-2,3,NH, Ahp-6- OH, NMePhe- NMe	2	54.0, CH	4.45, m	Tyr-1,3	Tyr-5,5',NH
NH		7.60, d (9.5)	NMePhe-1	Val-2,3,4,5, Ahp-6- OH, NMePhe-2, NMe	3	35.5, CH <sub>2</sub>	3.30, m	Tyr-2,4,5,5'	Tyr-3b,5,5',NH Tyr-3a,5,5',NH
NMePhe 1	169.3, C				4	128.4, C			
2	60.7, CH	5.05, dd (11.5,2.0)	NMePhe-3, NMe	NMePhe-5,5',6,6', Val-NH, Ile-2	5, 5'	129.8, CH	6.94, d (8.0)	Tyr-3,7	Tyr-2,3,6,6'
3	34.5, CH <sub>2</sub>	2.60, m	NMePhe- 2,4,5,5'	NMePhe- 3b,5,5',6,6'	6, 6'	115.2, CH	6.58, d (8.0)	Tyr-4,7	Tyr-5,5',7-OH
4	137.7, C	3.35, m	NMePhe-2	NMePhe-3a,5,5',6,6'	7	156.7, C			
5, 5'	129.7, CH	7.20, m	NMePhe- 3,7	NMePhe-2,3, Ile- 2,4,5	7-OH		9.13, brs		Tyr-6,6'
6, 6'	128.9, CH	7.25, m	NMePhe-4	NMePhe-2,3, Ile- 2,4,5	NH		8.51, d (8.7)	Tyr-2, Thr-1	Thr-2,3, Ahp-NH
7	126.6, CH	7.15, m	NMePhe- 5,5'	Val-4,5,NH	Thr 1	169.0, C			
NMe	30.5, CH <sub>3</sub>	2.56, s	NMePhe-2, Ile-1		2	54.7, CH	4.57, d (9.4)	Thr-1, Val-1	Thr-3,4,NH, Tyr- NH
Ile 1	170.1, C				3	72.1, CH	5.48, q (6.5)	Thr-4, Val-1	Tyr-2,NH, Ahp-NH
2	55.2, CH	4.37, d (10.4)	Ile-1,3,4,6, Ahp-6	Ile-3,4,6, NMePhe- 2,5,5',6,6'	4	17.7, CH <sub>3</sub>	1.15, d (6.5)	Thr-2,3	Thr-2,NH
3	34.4, CH	1.64, m	Ile-5,6	Ile-2,4a,5,6, Ahp-6, NPh-5,5',6,6'	NH		7.98, d (9.4)	Gln-1	Thr-2,4, Gln-2
4	24.5, CH <sub>2</sub>	0.13, ddq (13.5,6.8,7.2)	Ile-5,6	Ile-2,3,4b, NMe- Phe-5,5',6,6', Ile- 2,4a,5,6,	Gln 1	171.8, C			
5	12.2, CH <sub>3</sub>	0.53, t (7.2)	Ile-2,3,4	NMePhe-5,5',6,6'	2	51.6, CH	4.45, m	Gln-1,3,4	Gln-3,4,1-NH, Thr- NH
6	14.1, CH <sub>3</sub>	0.45, d (6.7)	Ile-3,4	Ile-3,4, NMePhe- 5,5',6,6'	3	28.6, CH <sub>2</sub>	1.73, m	Gln-1,2,4,5	Gln-2,1-NH
Ahp 2	169.5, C				4	31.5, CH <sub>2</sub>	2.10, m	Gln-2,3,5	Gln-2,1-NH
3	49.2, CH	4.46, m	Ahp-2,4	Ile-2,3,4	5	174.3, C			
4	21.8, CH <sub>2</sub>	1.72, m			NH		7.78, d (8.0)	Gln-2, Hpla-1	Gln-2,3,4,Hpla-2,2- OH
5	29.8, CH <sub>2</sub>	1.71, m			5-NH <sub>2</sub>		6.79, brs, 7.14, m	Gln-4	
		1.83, m			Hpla 1	173.5, C			
					2	72.7, CH	4.03, brd (7.5)		Hpla-3,5,5',2-OH, Gln-1-NH
					2-OH		5.51, brs	Hpla-2	Hpla-2, Gln-1-NH
					3	40.0, CH <sub>2</sub>	2.65, dd (14.0, 3.2)	Hpla-1,2,5,5'	Hpla-2,3b,5,5'
					4	128.6, C	2.49, m		Hpla-2,3a,5,5'
					5, 5'	130.4, CH	7.00, d (8.0)	Hpla-3,7	Hpla-2,3,6,6'
					6, 6'	114.9, CH	6.62, d (8.0)	Hpla-4,7	Hpla-5,5'
					7	156.5, C			
					7-OH		9.13, brs		

<sup>a</sup>500 MHz for <sup>1</sup>H, 125 MHz for <sup>13</sup>C. <sup>b</sup>Multiplicity and assignment from an HSQC experiment. <sup>c</sup>HMBC correlations, optimized for 8 Hz, are from the proton(s) stated to the indicated carbon. <sup>d</sup>Selected NOEs from ROESY experiment.

of the amino hydroxy piperidone (Ahp) and the *p*-hydroxyphenyllactic acid (Hpla) was suggested on the basis of the COSY and HSQC spectra, which presented the hydroxy proton at  $\delta_H$  6.04 coupled to the aminal proton at  $\delta_H$  4.90 (brs) ( $\delta_C$  74.2, CH) of the Ahp moiety, and the hydroxy proton  $\delta_H$  5.51 coupled to the oxymethine at  $\delta_H$  4.03 (brd) ( $\delta_C$  72.7, CH) for Hpla. Interpretation of the COSY, TOCSY, HSQC, and HMBC data (Table 1) allowed the assignment of the structure of eight residues: Val, NMePhe, *N,N*-disubstituted-Ile, Ahp, Tyr, Thr, Gln, and Hpla. The structure determination of the NMePhe moiety started with H-2, which resonated at  $\delta_H$  5.05 (dd) and was coupled through COSY correlations to a pair of benzylic protons (H-3,3',  $\delta_H$  2.60 and 3.35). An HSQC correlation established the connectivity of H-2 with an amino-methine carbon resonating at  $\delta_C$  60.7. The latter carbon exhibited HMBC

correlations with protons of an *N*-methyl resonating at  $\delta_H$  2.56 and the protons of methylene-3. HMBC correlations of C-3 and H-3 with the phenyl protons and carbons, respectively, established the connectivity of the phenyl ring to the aliphatic chain, and correlation of H-2 with the carbonyl, which resonated at  $\delta_C$  169.3, completed the structure elucidation of the NMePhe moiety. The doublet proton that resonated at  $\delta_H$  4.37 was assigned as the  $\alpha$ -proton of an isoleucine moiety on the basis of the COSY and TOCSY correlations, but failed to present any correlation with either an amine or amide proton. The carbonyl of the Ile  $\delta_C$  170.1 was assigned on the basis of its HMBC correlation with Ile-H-2. The correlation of the latter proton with the aminal carbon (Ahp-C-6) supported the establishment of this amino acid moiety as *N,N*-disubstituted-Ile. The sequence of these residues in **1**, Val-NMePhe-*N,N*-disubstituted-Ile-Ahp-Tyr-Thr-Gln-Hpla, and the



cyclization of the valine carbonyl to the threonine oxymethine could be independently assigned by the inter-residual HMBC or ROESY correlations (see Table 1). The relative configuration of the Ahp residue,  $3S^*,6R^*$ , was assigned on the basis of the similarity of its proton and carbon chemical shifts to those of micropeptin HM978 and the NOE of the pseudoaxial-H-4 (H-4<sub>pax</sub>,  $\delta_H$  2.51) with the 6-OH.<sup>13</sup> Marfey's analysis<sup>19</sup> (using L-FDAA as derivatizing reagent) preceded and not preceded by Jones' oxidation,<sup>20</sup> established the L-configuration of Glu  $\times$  2 (from Gln and from  $3S,6R$ -Ahp), Ile, NMePhe, Thr, Tyr, and Val, while analysis on a chiral-phase HPLC-column established the absolute configuration of Hpla as L. Comparison of the proton chemical shifts of the  $N,N$ -disubstituted-Ile of **1** with those of micropeptin HM978, both sharing similar chemical environments (Figure 1), revealed

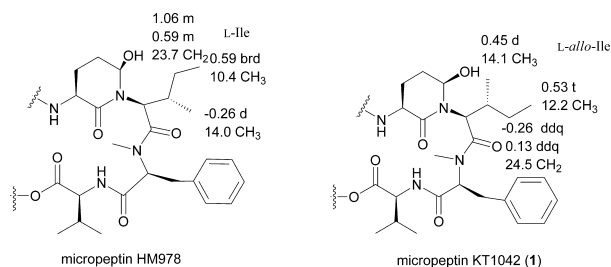


**Figure 1.** Comparison of the proton and carbon chemical shifts of the isoleucine moieties of micropeptins HM978 and KT1042 (1).

that the anisotropic effect of the neighboring aromatic ring is observed on the opposite arms of the isoleucine side chains in both compounds. The carbon chemical shifts of the  $N,N$ -di-

substituted-Ile in both compounds is significantly different, suggesting a different conformation or configuration at C-3. Because the L-FDAA reagent does not allow the discrimination of Ile from *allo*-Ile on a reversed-phase HPLC column, we repeated the analysis with the leucine amide derivative L-FDLA, which established the latter amino acid as L-*allo*-Ile. This established the structure of micropeptin KT1042 as **1**. Comparison of the proton and carbon chemical shifts of all  $N,N$ -disubstituted-Ile moieties in known micropeptins revealed that micropeptin KT1042 (**1**) is, so far, the only micropeptin that incorporates *allo*-Ile at this position. This finding also allowed concluding that, in the micropeptins, if an Ile is situated between the Ahp and the NMe-aromatic acid, the proton signal of 6-CH<sub>3</sub> will be shifted upfield of TMS, while in the case of *allo*-Ile, one of the 4-CH<sub>2</sub> protons will be shifted upfield of TMS. Because the conformation of the micropeptins in solution is quite rigid (due to the intramolecular hydrogen bonds between <sup>1</sup>Val-CO and <sup>4</sup>Ahp-NH and <sup>1</sup>Val-NH and <sup>4</sup>Ahp-6-OH), there is a significant difference in the carbon chemical shifts, as was observed by us previously, for these two amino acids when they occupy the C-terminus position of the micropeptins.<sup>21</sup>

Microguanidine KT636 (**2**) was isolated as a colorless oil. It presented a negative HRESIMS pseudomolecular ion at  $m/z$  635.1002, which matched the molecular formula, C<sub>19</sub>H<sub>32</sub>N<sub>4</sub>O<sub>14</sub>S<sub>3</sub>. The <sup>1</sup>H NMR spectrum of **2** in DMSO-*d*<sub>6</sub> (Table 2) was relatively broad, displaying signals characteristic of a 1,2,4-trisubstituted-phenyl ring ( $\delta_H$  7.16 dd, 7.24 d, 7.38 brd), five protons adjacent to electronegative substituents [ $\delta_H$  5.18 brs (2H), 4.93 d, 4.85 d, 4.14 d], a nine-proton singlet ( $\delta_H$  3.04), and a broad doublet methyl group ( $\delta_H$  1.18), reminiscent

**Table 2.** NMR Data of Microguanidine KT636 (**2**) in DMSO- $d_6$ <sup>a</sup>

position	$\delta_C$ , mult. <sup>b</sup>	$\delta_H$ , mult., J (Hz)	HMBC correlations <sup>c</sup>	NOE correlations <sup>d</sup>
Totpts 1	77.5, CH	5.18, brs	Totpts-2'	Totpts-3,2',5',6'
2	75.6, CH	5.18, brs	Totpts-2'	Totpts-3,2',5',6'
3	15.6, CH <sub>3</sub>	1.18, brd (2.0)	Totpts-1,2	Totpts-1,2,6'
1'	133.7, C			
2'	126.1, CH	7.38, brd (2.0)	Totpts-1,1',6',7'	Totpts-1,2,7', Me <sub>3</sub> -Arg-2
3'	129.7, C			
4'	149.5, C			
5'	120.6, CH	7.24, d (8.4)	Totpts-1',3',4',6'	Totpts-1,2
6'	125.9, CH	7.16, dd (8.4, 2.0)	Totpts-1,4'	Totpts-1,2,3
7'	63.1, CH <sub>2</sub>	4.93, d (13.9) 4.85, d (13.9)	Totpts-2',3',4'	Totpts-2' Totpts-2'
Me <sub>3</sub> -Arg 1	166.3, C			
2	73.5, CH	4.14, dd (11.2, 2.0)	Me <sub>3</sub> -Arg-1	Me <sub>3</sub> -Arg-3,4,5, Totpts-2'
3	23.1, CH <sub>2</sub>	1.85, m 2.05, m		Me <sub>3</sub> -Arg-2,5 Me <sub>3</sub> -Arg-2,5
4	23.4, CH <sub>2</sub>	1.22, m 1.36, m		Me <sub>3</sub> -Arg-2,5 Me <sub>3</sub> -Arg-2,5
5	40.0, CH <sub>2</sub>	3.08, m	Me <sub>3</sub> -Arg-3,4,6	Me <sub>3</sub> -Arg-2,3,4,5-NH
6	156.8, C			
7, 7', 7''	51.8, CH <sub>3</sub>	3.04, s	Me <sub>3</sub> -Arg-2	
5-NH		7.43, t (6.0)		Me <sub>3</sub> -Arg-5
6-NH, NH <sub>2</sub>		6.90, brs		

<sup>a</sup>400 MHz for <sup>1</sup>H, 100 MHz for <sup>13</sup>C. <sup>b</sup>Multiplicity and assignment from an HSQC experiment. <sup>c</sup>HMBC correlations, optimized for 8 Hz, are from the proton(s) stated to the indicated carbon. <sup>d</sup>Selected NOEs from ROESY experiment.

of the characteristic protons of microguanidine AL772, which was isolated and published by us several years ago.<sup>22</sup> The <sup>13</sup>C NMR spectrum revealed, among other signals, a carbonyl, guanidinium carbon, a trisubstituted phenyl moiety, three protons adjacent to electronegative substituents, an oxymethylene, and a trimethylammonium residue ( $\delta_C$  51.8, CH<sub>3</sub>). Interpretation of the COSY, TOCSY, HSQC, and HMBC data (Table 2) allowed the full assignment of the structure of 1-(4'-oxy-3'-(oxymethyl)phenyl)propane-1,2-dioxy-1,3',4'-tri-*O*-sulfate (tetraoxytolylpropane-trisulfate, Totpts) moiety and *N* $\alpha$ ,*N* $\alpha$ ,*N* $\alpha$ -trimethylarginine. The two moieties were linked together on the basis of comparison of the chemical shifts of the arginine carbonyl and C-2 of Totpts with that of microguanidine AL772<sup>22</sup> and the mass spectrometric data to assign structure **2** to microguanidine KT636.

Aeruginosins KT608A (**3**) and KT608B (**4**) were eluted closely one after the other from the reversed-phase HPLC column. They were isolated as a colorless oil with similar NMR spectra and identical molecular mass weights (Figures S3 and S4 in the Supporting Information). Both appeared as a ca. 1:1 mixture of the *cis* and *trans* rotamers of the amide bond between the Phe and Choi (57:43 *cis:trans* ratio in **3**, 54:46 *cis:trans* ratio in **4**). These rotamers were readily distinguished through the NOEs of Phe-H-2 with Choi-H-2 in the *cis* rotamer and of Phe-H-2 with Choi-H-7a in the *trans* rotamer.<sup>23</sup> Their specific rotations were found to be different,  $-53$  for **3** and  $+11$

for **4**. Full assignment of the <sup>1</sup>H and <sup>13</sup>C NMR data suggested that they presented opposite configurations at the stereogenic center of their Hpla moiety.

Aeruginosin KT608A (**3**) exhibited a positive HRESIMS molecular adduct ion at  $m/z$  609.3409 [M + H]<sup>+</sup>, consistent with the molecular formula C<sub>32</sub>H<sub>45</sub>N<sub>6</sub>O<sub>6</sub> and 14 degrees of unsaturation. The interpretation of the NMR data in DMSO- $d_6$  was rather complicated due to the high similarity of the chemical shifts of the proton and carbon signals of both rotamers. The <sup>1</sup>H NMR spectrum of **3** presented three pairs of amide protons (a pair of doublets and two pairs of triplets), two pairs of signals indicating the presence of a *para*-substituted phenol and a phenyl in the aromatic region, and four pairs of methine protons next to electronegative atoms in the 4.9–3.9 ppm region (Figure S3). The aliphatic region was too complicated to be interpreted. The <sup>13</sup>C NMR spectrum revealed three pairs of amide/ester carbonyls, two pairs of guanidine/phenol sp<sup>2</sup> carbons, 14 signals of aromatic sp<sup>2</sup> carbons consistent with two pairs of phenyl and phenol moieties, five pairs of methines between 73 and 50 ppm (Figure S4), and several additional methine and methylene signals in the aliphatic region. Both rotamers were fully characterized (Table 3, for the NMR data of the *cis* rotamer, and Table S3a in the Supporting Information for the *trans* rotamer), but for clarity only the structure elucidation of the major *cis* rotamer is discussed below. Interpretation of the data from the COSY, TOCSY, HSQC, and HMBC 2D NMR experiments allowed the assignment of the agmatine, Phe, and Hpla moieties (Table 3). The structure elucidation of the 2-carboxy-6-hydroxyoctahydroindole (Choi) moiety was more challenging. COSY and TOCSY correlations allowed the construction of the sequence of H-2 through H-7a, and the correlations in the HSQC spectrum allowed the assignment of the carbons bearing these protons (Table 3). H-2 exhibited COSY correlations with the adjacent protons resonating at  $\delta_H$  2.38 (a 9.5 Hz coupling constant) and 1.70 (<1 Hz) and NOEs with both of them, suggesting that the dihedral angles between H-2 and the *cis* proton resonating at  $\delta_H$  2.38 (H-3<sub>ax</sub>) and between H-2 and the *trans* proton resonating at  $\delta_H$  1.70 (H-3<sub>eq</sub>) are ca. 15° and ca. 90°, respectively. H-2 presented also an NOE with H-3a, which is coupled to H-3<sub>eq</sub> with a coupling constant of 6 Hz, suggesting that H-3a is *cis* oriented to H-2 in the pyrrolidine ring. H-3a exhibited an 8.0 Hz coupling constant and an NOE with H-7a, confirming their *cis* relationships. The above properties confirm the *cis* relationships of H-2, H-3a, and H-7a in the pyrrolidine ring.<sup>24</sup> In the cyclohexane ring, H-6 occupied an axial position on the basis of its large coupling constants (12.0 Hz) with H-5<sub>ax</sub> and H-7<sub>ax</sub> and its NOEs with H-5<sub>eq</sub>, H-7<sub>eq</sub>, and the axial H-7a. In the *trans* rotamer, H-7<sub>eq</sub> and H-7a exhibit NOEs with Phe-H-2, suggesting that Phe is *exo* oriented. The multiplicity of H-2 (doublet of 9.5 Hz) could thus be explained if the pyrrolidine ring adopts an envelope conformation where the nitrogen is out of the ring plane. Comparison of the Choi chemical shifts and multiplicities of the protons and carbons of **3** with those of microcin SF608 (containing L-Choi)<sup>14</sup> and aeruginosin EI461 (containing L-*diepi*-Choi)<sup>11,12</sup> (Figure 2) revealed that **3** exhibited NMR properties similar to those of the *diepi*-Choi moiety of aeruginosin EI461 except for the NOE between H-2 and H-3a. The arguments summarized above suggested that the relative configuration of the Choi moiety of **3** differs from that of aeruginosin EI461 or microcin SF608 and was consistent with either (2*S*,3*aS*,6*S*,7*aS*)- or (2*R*,3*aR*,6*R*,7*aR*)-Choi (L-6-*epi*-Choi or D-3*a*,7*a*-*diepi*-Choi, respectively, Figure 2). The sequence of the four subunits,

**Table 3. NMR Data of the Major *cis* Rotamer of Aeruginosin KT608A (3) in DMSO-*d*<sub>6</sub><sup>a</sup>**

position	$\delta_C$ , mult. <sup>b</sup>	$\delta_H$ , mult., <i>J</i> (Hz)	HMBC correlations <sup>c</sup>	NOE correlations <sup>d</sup>
Agm 1	38.6, CH <sub>2</sub>	3.18, m 3.06, m	Agm-2, Choi-1	Agm-1-NH
2	26.2, CH <sub>2</sub>	1.45, m	Agm-3,4	Agm-1-NH
3	26.4, CH <sub>2</sub>	1.41, m	Agm-3	Agm-4-NH
4	40.6, CH <sub>2</sub>	3.08, m	Agm-3,5	Agm-4-NH
5	156.9, C			
1-NH		8.29, t (5.5)	Agm-1, Choi-1	Agm-1,2, Choi-2,3eq
4-NH		7.52, t (5.5)	Agm-4	Agm-3,4
Choi 1	172.3, C			
2	59.6, CH	4.82, d (9.5)	Choi-1,3ax,3a	Choi-3ax,3eq,3a, Phe-2,3, Agm-1-NH
3	33.6, CH <sub>2</sub>	2.38, m (ax) 1.70, dd (12.0, 6.0)	Choi-1,3a,7a	Choi-2,3a,5ax, Phe-2 Choi-2, Agm-1-NH
3a	32.7, CH	2.23, m	Choi-2,4	Choi-2,3ax,7a
4	22.7, CH <sub>2</sub>	1.63, m (2H)	Choi-6	
5	29.9, CH <sub>2</sub>	1.56, m (eq) 1.19, m (ax)		Choi-6 Choi-3ax
6	67.0, CH	3.30, m		Choi-5eq,7eq,7a
7	36.1, CH <sub>2</sub>	2.37, m (eq)	Choi-3a	Choi-6,7ax,7a
7a	56.8, CH	0.83, q (12.0) 4.04, ddd (12.0, 8.0, 6.5)	Choi-5,6,7a Choi-2,3	Choi-7eq Choi-3a,6,7eq
Phe 1	170.0, C			
2	51.8, CH	4.20, m	Phe-1,3, Hpla-1	Phe-3,5,5',NH, Choi-2,3ax
3	36.5, CH <sub>2</sub>	2.84, m 2.81, m	Phe-1,2,5,5'	Phe-2,NH Phe-2,NH
4	138.4, C			
5, 5'	129.2, CH	7.12, d (7.0)	Phe-3,5',5,7	Phe-2
6, 6'	128.2, CH	7.19, t (7.0)	Phe-4,6',6	
7	126.4, CH	7.14, t (7.0)	Phe-5,5'	
NH		7.97, d (8.0)	Phe-2,3, Hpla-1	Phe-2,3, Hpla-2,3
Hpla 1	173.5, C			
2	72.0, CH	3.85, dd (9.0, 3.5)	Hpla-1,3	Hpla-3,5,5',2-OH, Phe-NH
3	39.5, CH <sub>2</sub>	2.33, m 2.55, dd (14.0, 3.5)	Hpla-1,2,5,5' Hpla-5,5'	Hpla-3,5,5', Phe-NH Hpla-3,5,5', Phe-NH
4	128.5, C			
5, 5'	130.4, CH	6.82, d (8.4)	Hpla-3,5',5,6,6',7	Hpla-2,3
6, 6'	114.9, CH	6.57, d (8.4)	Hpla-4,5,5',6,6',7	Hpla-7-OH
7	155.7, C			
2-OH		5.05, brs		Hpla-2
7-OH		9.06, brs		Hpla-6,6'

<sup>a</sup>400 MHz for <sup>1</sup>H, 100 MHz for <sup>13</sup>C. <sup>b</sup>Multiplicity and assignment from an HSQC experiment. <sup>c</sup>HMBC correlations, optimized for 8 Hz, are from the proton(s) stated to the indicated carbon. <sup>d</sup>Selected NOEs from ROESY experiment.

Hpla-Phe-*diepi*-Choi-agmatine, was determined on the basis of the HMBC correlations of Hpla-CO with Phe-NH and H-2, NOE correlations of Phe-H-2 and Choi-H-2, and HMBC correlation of Choi-CO with agmatine-NH. This established the planar structure of 3 and the relative configuration of the Choi moiety.

**Table 4. NMR Data of the Major *cis* Rotamer of Aeruginosin KT608B (4) in DMSO-*d*<sub>6</sub><sup>a</sup>**

position	$\delta_C$ , mult. <sup>b</sup>	$\delta_H$ , mult., <i>J</i> (Hz)	HMBC correlations <sup>c</sup>	NOE correlations <sup>d</sup>
Agm 1	38.6, CH <sub>2</sub>	3.07, m 3.19, m	Agm-2,3, Choi-1	Agm-1-NH
2	26.2, CH <sub>2</sub>	1.45, m	Agm-3,4	
3	26.4, CH <sub>2</sub>	1.41, m	Agm-2	
4	40.5, CH <sub>2</sub>	3.07, m	Agm-3,5	Agm-4-NH
5	156.9, C			
1-NH		8.20, t (5.2)	Agm-1, Choi-1	Agm-1, Choi-2
4-NH		7.62, brs		Agm-4
Choi 1	172.3, C			
2	59.5, CH	4.80, d (8.8)	Choi-1,3ax,3a,7a	Choi-3ax,3eq,3a, Phe-2, Agm-1-NH
3	33.8, CH <sub>2</sub>	2.35, m (ax) 1.70, dd (12.0,6.0)	Choi-1,3a,4,7a	Choi-2,3a,5ax,7a Choi-2
3a	32.7, CH	2.22, m	Choi-2,4	Choi-3ax,7a
4	22.7, CH <sub>2</sub>	1.60, m (2H)		
5	29.9, CH <sub>2</sub>	1.55, m (eq) 1.17, m (ax)		Choi-6 Choi-3c
6	67.0, CH	3.30, m		Choi-5eq,7eq,7a
7	36.2, CH <sub>2</sub>	2.35, m (eq)	Choi-5,6	Choi-6,6-OH,7ax,7a
7a	56.8, CH	0.83, q (12.0) 4.05, ddd (12.0, 8.2, 5.6)	Choi-3a,7a	Choi-6-OH,7eq
6-OH		4.53, d (6.4)		Choi-7ax,7eq
Phe 1	170.0, C			
2	51.4, CH	4.26, m	Phe-1,4, Hpla-2	Phe-3,5,5',NH, Choi-2,3ax
3	36.5, CH <sub>2</sub>	2.80, m 2.81, m	Phe-1,2,4,5,5' Phe-1,2,5,5'	Phe-2,NH Phe-2,NH
4	138.2, C			
5,5'	129.2, CH	7.10, d (7.0)	Phe-3,5',5,7	Phe-2
6,6'	128.2, CH	7.22, m	Phe-4,6',6	
7	126.4, CH	7.16, m	Phe-5,5'	
NH		7.97, d (8.0)	Hpla-1	Phe-2,3, Hpla-2,3
Hpla 1	173.4, C			
2	72.3, CH	3.88, m	Hpla-1,3,4	Hpla-3,5,5',2-OH, Phe-NH
3	39.7, CH <sub>2</sub>	2.29, m 2.60, dd (14.0,3.6)	Hpla-1,2,4,5,5' Hpla-1	Hpla-2-OH,3,5,5' Hpla-2-OH,3,5,5'
4	128.4, C			
5, 5'	130.3, CH	6.85, d (8.4)	Hpla-3,4,5,5',6,6',7	Hpla-2,3
6, 6'	114.9, CH	6.58, d (8.4)	Hpla-5,5',6,6',7	Hpla-7-OH
7	155.7, C			
2-OH		5.31, d 6.4	Hpla-1	Hpla-2,3
7-OH		9.10, brs	Hpla-7-OH	Hpla-6,6'

<sup>a</sup>400 MHz for <sup>1</sup>H, 100 MHz for <sup>13</sup>C. <sup>b</sup>Multiplicity and assignment from an HSQC experiment. <sup>c</sup>HMBC correlations, optimized for 8 Hz, are from the proton(s) stated to the indicated carbon. <sup>d</sup>Selected NOEs from ROESY experiment.

Aeruginosin KT608B (4) presented similar <sup>1</sup>H and <sup>13</sup>C NMR data (Tables 4 and S4a) and an identical molecular ion in the HRESI mass spectrum (*m/z* 609.3400, [M + H]<sup>+</sup>) to 3. Analysis of the 2D NMR data revealed that 4 has the same four subunits, Hpla, Phe, *diepi*-Choi, and agmatine, and that they are

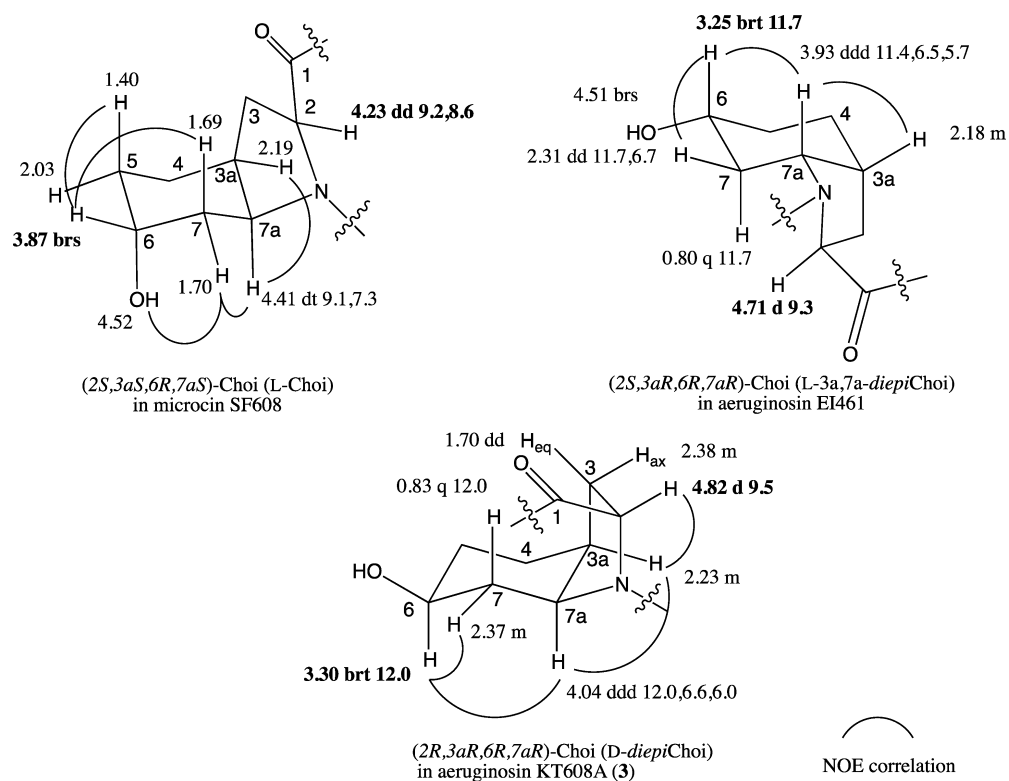


**Figure 2.** Comparison of the chemical shifts, coupling constants, and NOEs of the different Choi isomers.

assembled in the same linear order as **3**. Careful comparison of the  $^1\text{H}$  and  $^{13}\text{C}$  NMR data of **3** and **4** revealed some minor differences in chemical shifts of C-2 of the Hpla units and the Phe-NH signals (Figures S3 and S4). These differences suggested that either the Phe or Hpla differ in their absolute configuration in **3** and **4**. Applying Marfey's method (L-FDAA) and chiral-phase HPLC, as discussed above for **1**, revealed that the D-Phe and *diepi*-Choi were similar in both compounds, while the Hpla moiety was L in **3** and D in **4**. The retention times of *diepi*-Choi-L-FDAA (31.0 min), from **3** and **4**, were significantly shorter than those of the L-Choi-L-FDAA (38.1 min) and L-6-*epi*-Choi-L-FDAA (36.6 min) standards we used for comparison (Figures S5 and S6, respectively). In order to establish the absolute configuration of the new *diepi*-Choi, we derivatized the hydrolysate of **4** with D-FDAA and compared the retention times of the two pairs of derivatives, according to the procedure of the advanced Marfey's method<sup>25</sup> (Figure S7). The retention times of *diepi*-Choi-L-FDAA and *diepi*-Choi-D-FDAA from **4** were 31.0 and 29.4 min, respectively, suggesting that this *diepi*-Choi moiety was of the D series and thus had the (2R,3aR,6R,7aR) absolute configuration. This established the structures of aeruginosin KT608A and aeruginosin KT608B as **3** and **4**, respectively.

Aeruginosin KT650 (**5**) was isolated as a transparent oil, which exhibited a HR MALDI-TOF-MS molecular cluster ion ( $[\text{M} + \text{Na}]^+$ ) at  $m/z$  673.3320, consistent with the molecular formula  $\text{C}_{34}\text{H}_{46}\text{N}_6\text{O}_7$  and 15 degrees of unsaturation. Similar to the other aeruginosins, it appeared in the NMR spectra as a 3:2 mixture of the *cis* and *trans* rotamers. The NMR data of **5** (Tables 5 and S5a) were similar to those of **3** and **4** (Tables 3 and 4) except for changes in the chemical shifts of the Phe-NH, which resonated in **5** ca. 0.5 ppm downfield compared to those of **3** and **4**, the Hpla H-2, which resonated ca. 1 ppm downfield of those of **3** and **4**, the Hpla C-2, which resonated ca. 1.5 ppm

downfield of those for **3** and **4**, the Hpla C-3, which resonated ca. 3 ppm upfield, and the presence of additional acetyl signals in the NMR spectra of **5** ( $\delta_{\text{H}}$  1.87, s;  $\delta_{\text{C}}$  169.7, C; 20.7,  $\text{CH}_3$ ). Analysis of the 2D NMR data (including N-H HSQC and HMBC experiments) revealed that **5** was the Hpla-2-O-acetyl derivative of **3** or **4**. The absolute configurations of the acid units were analyzed as described above for **3** and **4**, revealing that the absolute configurations of *diepi*-Choi, Phe, and Hpla were D, thus establishing the structure of aeruginosin KT650 as **5**.

Pseudoaeruginosin KT554 (**6**) was isolated as a glassy solid from the cell-mass extract. In the HRESIMS, it presented a protonated molecular ion cluster ( $[\text{M} + \text{H}]^+$ ) at  $m/z$  555.3280, confirming its molecular formula  $\text{C}_{29}\text{H}_{43}\text{N}_6\text{O}_5$  and 12 degrees of unsaturation. Contrary to aeruginosins **3**–**5** the NMR spectra of **6** displayed a single isomer. Interpretation of the data from the 1D  $^1\text{H}$  and  $^{13}\text{C}$  NMR spectra and COSY, TOCSY, HSQC, and HMBC 2D NMR experiments allowed the assignment of the agmatine, Phe, Leu, and Hpla moieties (Table 6). The assembly of the short peptide sequence was achieved by interpretation of the HMBC and ROESY correlations (Table 6), while Marfey's procedure<sup>18</sup> and chiral-phase HPLC established **6** as D-Hpla-D-Leu-L-Phe-agmatine. We termed this metabolite as pseudoaeruginosin KT554 because we believe that it was derived from a distorted biosynthetic pathway similar to the one that produces **3**–**5**, as described below.

Aeruginosin GH553 (**7**) was isolated as a glassy solid from bloom material that was collected from a fishpond in Kibbutz Giva'at Haim on November 2003.<sup>13</sup> High-resolution MALDI-TOF-MS measurements of its sodiated molecular cluster ion at  $m/z$  576.2354 established the molecular formula of **7** as  $\text{C}_{29}\text{H}_{35}\text{N}_3\text{O}_8$ . The  $^1\text{H}$  NMR spectrum of **7** in  $\text{DMSO}-d_6$  (Tables 7 and S7a) revealed that it was composed of three acid units and appears as a 1:1 mixture of two conformers, characteristic of the *cis* and *trans* rotamers of the aeruginosins. As in the case of aeruginosin

Table 5. NMR Data of the Major *cis* Rotamer of Aeruginosin KT650 (5) in DMSO- $d_6^a$ 

position	$\delta_{C/N}$ , mult. <sup>b</sup>	$\delta_H$ , mult., J (Hz)	HMBC correlations <sup>c</sup>	NOE correlations <sup>d</sup>
Agm 1	38.6, CH <sub>2</sub>	3.14, m 3.02, m	Agm-2,3 Agm-2,3	Agm-1-NH
2	26.1, CH <sub>2</sub>	1.44, m	Agm-3,4	Agm-1-NH,4-NH
3	26.4, CH <sub>2</sub>	1.40, m	Agm-2	Agm-1-NH,4-NH
4	41.0, CH <sub>2</sub>	3.08, m	Agm-5	Agm-4-NH
5	156.9, C			
1-NH	113.0, NH	8.18, t (5.4)	Agm-1, Choi-1	Agm-1,2,3, Choi-2
4-NH	85.0, NH	7.62, brs		Agm-2,3,4
5-NH <sub>2</sub>	35.0, NH <sub>2</sub>	7.20, m		
Choi 1	172.3, C			
2	59.4, CH	4.78, d (9.2)	Choi-3a,7a	Choi-3ax,3eq,3a, Phe-2, Agm-1-NH
3	33.5, CH <sub>2</sub>	2.31, m (ax) 1.68, dd (12.0, 6.0)	Choi-3a Choi-7a	Choi-2,3a,5ax Choi-2, 6
3a	32.8, CH	2.18, m	Choi-2,3	Choi-2,3ax,6
4	22.7, CH <sub>2</sub>	1.62, m (2H)		Choi-5ax
5	29.9, CH <sub>2</sub>	1.55, m (eq) 1.18, m (ax)		Choi-4,6 Choi-3c,4
6	67.0, CH	3.35, m		Choi-5eq,7eq,7a
7	35.7, CH <sub>2</sub>	2.34, m (eq) 0.83, q (11.8)	Choi-6,7a	Choi-6,7ax,7a Choi-6,7eq,7a
7a	56.5, CH	4.03, ddd (11.8, 8.2, 5.3)	Choi-2	Choi-3c,3a,6,7eq
6-OH		4.55, brs		
8-N	140.2, <i>ter</i> N			
Phe 1	170.0, C			
2	52.0, CH	4.17, m	Phe-3	Phe-5,5',NH, Choi-2,3ax
3	35.9, CH <sub>2</sub>	2.86, m 2.87, m	Phe-1,2,5,5' Phe-1,2,4	Phe-2,NH Phe-2,NH
4	138.5, C			
5, 5'	129.2, CH	7.20, m	Phe-3,5',5,7	Phe-2
6, 6'	128.2, CH	7.23, m	Phe-4,6',6,	
7	126.4, CH	7.21, m	Phe-5,5',6,6'	
NH	119.5, NH	8.48, d (7.9)	Phe-3, Hpla-1	Phe-2,3, Hpla-2
Hpla 1	169.2, C			
2	73.8, CH	4.90, dd (8.8,4.0)	Hpla-3b	Hpla-3,5,5', Ac-CH <sub>3</sub> , Phe-NH
3	36.5, CH <sub>2</sub>	2.83, m (a) 2.61, dd (14.0, 8.8)	Hpla-4,5,5' Hpla-1	Hpla-2,5,5' Hpla-2,5,5'
4	126.9, C			
5, 5'	130.3, CH	6.92, d (8.4)	Hpla-3,5',5,6,6',7	Hpla-2,3
6, 6'	115.2, CH	6.65, d (8.4)	Hpla-4,5,5',6,6',7	
7	156.1, C			
7-OH		9.18, brs		
Ac-CO	169.7, C			
Ac-CH <sub>3</sub>	20.7, CH <sub>3</sub>	1.87, s	Ac-CO	Hpla-2

<sup>a</sup>400 MHz for <sup>1</sup>H, 100 MHz for <sup>13</sup>C. <sup>b</sup>Multiplicity and assignment from an HSQC experiment. <sup>c</sup>HMBC correlations, optimized for 8 Hz, are from the proton(s) stated to the indicated carbon. <sup>d</sup>Selected NOEs from ROESY experiment.

KT650 (5), aeruginosin GH553 (7) exhibited an absorption line of an acetate group ( $\delta_H$  1.99 for the *cis* rotamer and 1.95 for the *trans* rotamer). Analysis of the COSY, TOCSY, HSQC, and HMBC 2D

Table 6. NMR Data of Pseudoaeruginosin KT554 (6) in DMSO- $d_6^a$ 

position	$\delta_C$ , mult. <sup>b</sup>	$\delta_H$ , mult., J (Hz)	HMBC correlations <sup>c</sup>	NOE correlations <sup>d</sup>
Agm 1	38.2, CH <sub>2</sub>	3.00, m 3.08, m	Agm-2 Agm-2	Agm-1-NH Agm-1-NH
2	26.0, CH <sub>2</sub>	1.40, m 1.23, m		
3	26.3, CH <sub>2</sub>	1.40, m		
4	41.0, CH <sub>2</sub>	3.10, m	Agm-3,5	Agm-4-NH
5	156.8, C			
1-NH		7.96, t (5.2)	Phe-1	Agm-1, Phe-2
4-NH		7.48, t (5.0)		Agm-4
Phe 1	171.1, C			
2	54.4, CH	4.38, ddd (16.0,8.4,4.0)		Phe-NH, Agm-1-NH
3	37.8, CH <sub>2</sub>	3.01, dd (13.5,5.2) 2.71, dd (13.5, 11.1)	Phe-4,5,5' Phe-2,4,5,5'	Phe-5,5' Phe-NH
4	138.0, C			
5,5'	129.3, CH	7.22, m	Phe 4,6,6',7	Phe 3a, Leu3,5,6
6,6'	128.1, CH	7.23, m	Phe-4,7	Phe-3a, Leu-3,5,6
7	126.3, CH	7.10, m		Leu-5,6
NH		8.38, d 8.8	Leu-1	Phe-3a, Leu-3,5,6
Leu 1	171.8, C			
2	50.8, CH	4.21, q (6.8)	Leu-1,3,4	Leu-NH, Phe-NH
3	41.6, CH <sub>2</sub>	1.05, t (5.2)		Leu-NH, Phe-5,5',6,6',NH
4	23.8, CH	1.00, m	Leu-5,6	Leu-NH
5	22.9, CH <sub>2</sub>	0.67, d (6.0)	Leu-3,4	Leu-NH, Phe-5,5',6,6',7,NH
6	22.2, CH <sub>2</sub>	0.67, d (6.0)	Leu-3,4	Phe-5,5',6,6',7,NH
NH		7.38, d (8.0)	Hpla-1	Leu-2,3,4,5,6, Hpla-2,2-OH
Hpla 1	173.0, C			
2	72.2, CH	4.00, ddd (7.6, 7.2, 5.2, 4.0)		Leu-NH
3	40.0, CH <sub>2</sub>	2.82, dd (14.0, 7.6) 2.59, dd (14.0, 7.2)	Hpla-2,4,5,5'	Hpla-6,6',NH Hpla-6,6',NH
4	128.3, C			
5,5'	130.5, CH	6.96, d (8.3)	Hpla-7	
6,6'	114.8, CH	6.60, d (8.3)	Hpla-4,6',6,7	Hpla-3
7	155.8, C			
2-OH		5.57, d (5.2)		Leu-NH
7-OH		9.09, brs	Hpla-6,6',7	

<sup>a</sup>500 MHz for <sup>1</sup>H, 125 MHz for <sup>13</sup>C. <sup>b</sup>Multiplicity and assignment from an HSQC experiment. <sup>c</sup>HMBC correlations, optimized for 8 Hz, are from the proton(s) stated to the indicated carbon. <sup>d</sup>Selected NOEs from ROESY experiment.

NMR spectra (Tables 7 and S7a) allowed the assignment of the three acid units that composed 7, Choi-amide-6-acetate, tyrosine, and Hpla. The Choi-H-6 coupling constants (dddd, 11.6, 11.6, 4.0, 4.0 Hz) suggested its axial orientation in a cyclohexane bearing a chair conformation. This was indeed confirmed by the NOEs of H-6 with axial H-4 and H-7a and equatorial H-5 and H-7. Comparison of the proton and carbon chemical shifts of the Choi moiety in 7 with that of 3 suggested that the conformation of the *cis*-fused octahydroindole moiety in both compounds was similar and that

the acetate was attached to the oxygen on C-6 on the basis of the chemical shift of H-6 ( $\delta_{\text{H}}$  4.52 in **7** versus 3.30 in aeruginosin KT608A). NOEs of the acetate methyl group with the adjacent Choi protons supported this suggestion. Further analysis of the coupling constant and NOE correlations revealed that the relative configuration of C-2 of the Choi moiety in **7** was identical to that of **3** due to the observed NOE between H-2 and H-3a. Marfey's analysis<sup>25</sup> using L-FDAA and D-FDAA as the coupling reagents established the D-configuration of Tyr and *diepi*-Choi (2*R*,3*aR*,6*R*,7*aR*-Choi). Analysis of the Hplc on a chiral-phase HPLC column established its absolute configuration as L. On the basis of the results discussed above, the structure of aeruginosin GH553 was assigned as **7**.

**Biological Activities.** The extracts of strain IL-347 exhibited significant inhibition of the serine proteases trypsin and chymotrypsin at a concentration of 1 mg/mL. The activity-guided purification of the protease-inhibiting components of the extract revealed that micropeptides KT1042 (**1**) and HM978 were responsible for the inhibition of chymotrypsin, while micropeptide SF909, cyanopeptolin S, aeruginosins KT608A (**3**), KT608B (**4**), and KT650 (**5**), and pseudoaeruginosin KT554 (**6**) were responsible for the inhibition of trypsin.

The inhibitory activities of **1–7** were determined for the serine protease trypsin, thrombin, chymotrypsin, and elastase. Micropeptide KT1042 (**1**) inhibited chymotrypsin with an  $\text{IC}_{50}$  of 0.26  $\mu\text{M}$  but not trypsin, thrombin, or elastase at a concentration of 45.5  $\mu\text{M}$ . Microguanidine KT636 (**2**) was assayed for the inhibition of trypsin, thrombin, and bovine amino peptidase N at a concentration of 45.5  $\mu\text{M}$  and found not active. It was also not active in a cytotoxicity assay against the HCT116 cell line at a concentration of 1.6  $\mu\text{M}$ . Aeruginosin KT608A (**3**) inhibited trypsin with an  $\text{IC}_{50}$  of 1.9  $\mu\text{M}$  but enhanced the activity of thrombin by 30% at a concentration of 45.5  $\mu\text{M}$ . Aeruginosin KT608B (**4**) inhibited trypsin with an  $\text{IC}_{50}$  of 1.3  $\mu\text{M}$  and thrombin by less than 50% at a concentration of 45.5  $\mu\text{M}$ . Aeruginosin KT650 (**5**) inhibited trypsin with an  $\text{IC}_{50}$  of 19.9  $\mu\text{M}$  and inhibited thrombin activity by less than 50% at a concentration of 45.5  $\mu\text{M}$ . Pseudoaeruginosin KT554 (**6**) and aeruginosin GH553 (**7**) inhibited trypsin with  $\text{IC}_{50}$  values of 45.5  $\mu\text{M}$ , but not thrombin at the same concentration. Compounds **3–7** did not inhibit chymotrypsin and elastase at a concentration of 45.5  $\mu\text{M}$ .

**Concluding Remarks.** Micropeptide KT1042 (**1**) and micropeptide HM978 share a very similar amino acid sequence, cyclo-(<sup>1</sup>Val-<sup>2</sup>NMePhe-<sup>3</sup>Ile-<sup>4</sup>Ahp-<sup>5</sup>X-<sup>6</sup>Thr)-<sup>7</sup>Asn-<sup>8</sup>Hpla. Despite this structural similarity, the proton and carbon chemical shifts of the 3Ile, which are affected by the <sup>2</sup>NMePhe ring current, were significantly different. This observation led us to the finding that the chemical shifts of the carbons and protons in the side chains of Ile and *allo*-Ile in the micropeptides may effortlessly distinguish one from the other.

Aeruginosins **3–5** and **7** compose a new subgroup of aeruginosins that contain a new stereoisomer of the Choi core. This isomer, 2*R*,3*aR*,6*R*,7*aR*-Choi (D-3*a*,7*a*-*diepi*-Choi), adds to the two known isomers (2*S*,3*aS*,6*R*,7*aS*)-Choi (L-Choi) and (2*S*,3*aR*,6*R*,7*aR*)-Choi (L-3*a*,7*a*-*diepi*-Choi). Scheme 1 summarizes the biogenesis steps that start with L-arogenate and lead to the different Choi isomers. The scheme is based on the biogenetic pathway for L-Choi (upper trace) suggested by Ishida et al., based on the enzymatic functions deduced from the ORFs in the aeruginoside 126 biosynthetic gene cluster.<sup>26</sup> There are two possible routes to the biosynthesis of D-3*a*,7*a*-*diepi*-Choi. One is derived from the same L-arogenate oxidation product as L-Choi in

**Table 7. NMR Data of the Major *cis* Rotamer of Aeruginosin GH553 (**7**) in DMSO-*d*<sub>6</sub><sup>a</sup>**

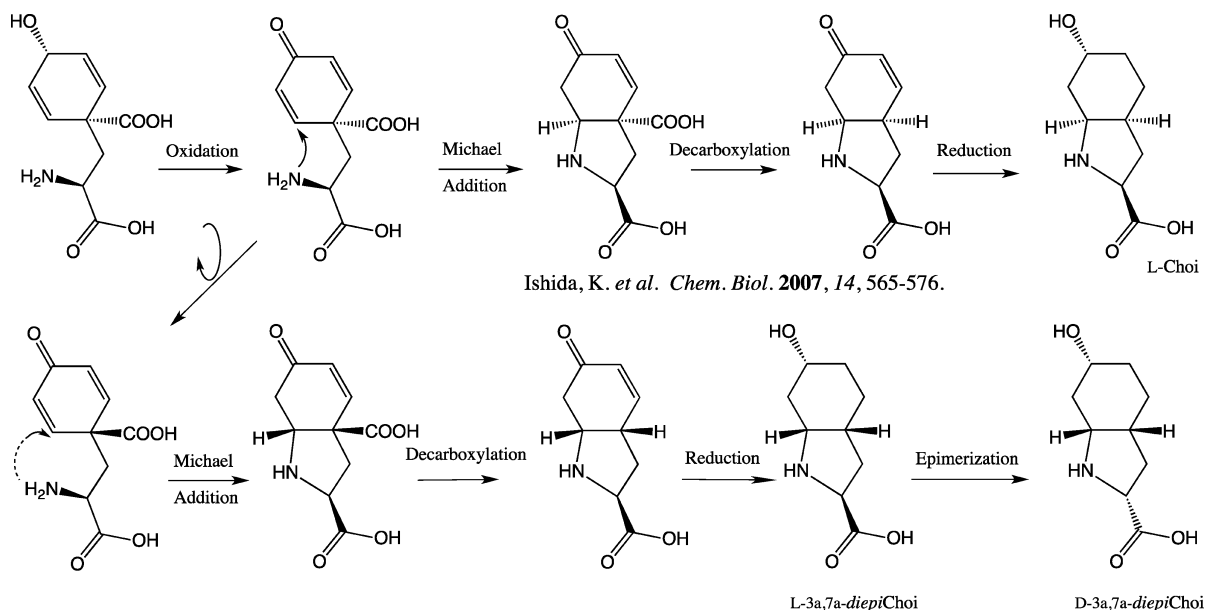
position	$\delta_{\text{C}}$ , mult. <sup>b</sup>	$\delta_{\text{H}}$ , mult., <i>J</i> (Hz)	HMBC correlations <sup>c</sup>	NOE correlations <sup>d</sup>
Choi 1	174.2, C			
2	59.3, CH	4.76, d (9.1)	Choi-3,4,7a	Choi-3ax,3eq,7ax, NH, Tyr-2
3	33.1, CH <sub>2</sub>	2.42, m (ax) 1.77, m		Choi-2 Choi-2,3a,NHb
3a	32.7, CH	2.31, m	Choi-4	Choi-3ax,7a, Ac-CH <sub>3</sub>
4	22.2, CH <sub>2</sub>	1.71, m (eq) 1.65, m	Choi-3	Choi-6,7a
5	26.0, CH <sub>2</sub>	1.66, m (eq) 1.48, m (ax)	Choi-7a	Choi-6
6	70.6, CH	4.52, tt (11.6,4.0)		Choi- 4ax,5eq,7eq,7a
7	32.1, CH <sub>2</sub>	2.46, m (eq) 1.02, q (12.2)	Choi-5,6,7a	Choi-6,7ax,7a Choi-2,7eq
7a	56.2, CH	4.11, m		Choi-3a,4ax,6,7eq
1-NHa		7.31, s	Choi-2	
1-NHb		7.74, s	Choi-1	Choi-2,3ax
Ac-CO	169.8, C			
Ac-CH <sub>3</sub>	21.1, CH <sub>3</sub>	1.97, s	Ac-CO	Choi-3a
Tyr 1	170.4, C			
2	52.0, CH	4.18, brq (8.8)	Tyr-1,3	Tyr-3,5,5',NH, Choi-2
3	35.8, CH <sub>2</sub>	2.80, m 2.62, m	Tyr-2,4,5,5'	Tyr-2,5,5',NH Tyr-2,5,5'
4	128.6, C			
5, 5'	130.5, CH	6.97, d (8.4)	Tyr-5,5,7	Tyr-2,3
6, 6'	115.0, CH	6.59, d (8.4)	Tyr-4,7	
7	155.9, C	7.16, m		
NH		7.62, d (7.7)	Tyr-2, Hpla-1	Tyr-2,3a, Hpla-2,3a
7-OH		9.10, s	Tyr-6,6',7	
Hpla 1	173.3, C			
2	72.4, CH	3.85, dd (8.6,4.0)		Hpla-3,5,5', Tyr-NH
3	39.5, CH <sub>2</sub>	2.31, m 2.60, m	Hpla- 1,2,4,5,5'	Hpla-2,5,5'
4	128.6, C			
5, 5'	130.3, CH	6.86, d (8.4)	Hpla-7	Hpla-2,3
6, 6'	114.9, CH	6.57, d (8.4)	Hpla-4,6',6,7	
7	155.7, C			
2-OH		5.25, brs		
7-OH		9.06, brs	Hpla-6,6',7	

<sup>a</sup>400 MHz for <sup>1</sup>H, 100 MHz for <sup>13</sup>C. <sup>b</sup>Multiplicity and assignment from an HSQC experiment. <sup>c</sup>HMBC correlations, optimized for 8 Hz, are from the proton(s) stated to the indicated carbon. <sup>d</sup>Selected NOEs from ROESY experiment.

which the Michael addition of the amine to the conjugated double bond occurs after a 180-degree rotation of the six-membered ring to afford the L-3*a*,7*a*-*diepi*-cyclization product. The rest of the steps are identical to those proposed for L-Choi, establishing the L-3*a*,7*a*-*diepi*-Choi. An additional epimerization step affords the D-3*a*,7*a*-*diepi*-Choi that is contained in **3–5** and **7**. The second possible route to D-3*a*,7*a*-*diepi*-Choi may involve an initial inversion of L-arogenate to D-arogenate followed by a Michael addition to afford the D-3*a*,7*a*-*diepi*-cyclization product, which in turn is decarboxylated and reduced to afford the all-R, D-3*a*,7*a*-*diepi*-Choi.



Scheme 1. Proposed Biogenesis of the New Aeruginosins



Pseudoaeruginosin KT554 (**6**) is proposed to be derived from an altered gene cluster that contains, instead of the L-arogenate-oxidizing enzyme, an enzyme that converts arogenate to phenylalanine (probably the one that is used by the cyanobacteria for the primary production of phenylalanine), leading after the assembly of all four biosynthetic units to the short peptide **6** we termed pseudoaeruginosin KT554. The proposed line of enzymatic processes demonstrates the versatility of the biosynthetic machinery utilized by cyanobacteria for the synthesis of secondary metabolites. This strategy allows cyanobacteria to produce peptide-mimicking building blocks that interfere with the degradation of these short peptides.

## EXPERIMENTAL SECTION

**General Experimental Procedures.** Optical rotations were measured on a JASCO P-1010 polarimeter. UV spectra were recorded on an Agilent 8453 spectrophotometer. NMR spectra were recorded on a Bruker DMX-500 spectrometer at 500.13 MHz for  $^1\text{H}$  and 125.76 MHz for  $^{13}\text{C}$  and a Bruker Avance 400 spectrometer at 400.13 MHz for  $^1\text{H}$  and 100.62 MHz for  $^{13}\text{C}$ . DEPT, COSY-45, gTOCSY, gROESY, gHSQC, gHMBC, and gHMBC spectra were recorded using standard Bruker pulse sequences. High-resolution MS were recorded on an Applied Biosystems Voyager System 4312 instrument and a Waters MALDI Synapt instrument. HPLC separations were performed on a Jasco HPLC system (model PU-2080 Plus pump, model LG-2080-04 quaternary gradient unit, and model PU-2010 Plus multiwavelength detector), a Merck HPLC system (model L-6200A pump and model L-4200 UV-vis detector), and a Merck Hitachi HPLC system (L-7000A intelligent pump and model L-6200 UV-vis detector). An Eliza EL<sub>x</sub>808 reader (Bio-Tek Instruments, Inc.) was used for protease inhibition assays.

**Biological Material.** *Microcystis aeruginosa*, TAU strain IL-347, was collected in March 2005, from Lake Kinneret, Israel. The aqueous solution containing the cells was left for aggregation with alum overnight. The cell mass was separated from aqueous solution, and the cell mass was frozen and lyophilized. Samples of the cyanobacteria are deposited at the culture collection of Tel Aviv University.

**Isolation Procedure.** The brown-colored aqueous solution (12 L) was loaded on an Amberlite XAD-2 column (1 kg), and the adsorbed organic material was eluted from the column with MeOH (3 L). The MeOH extract (1 g) was separated by gel filtration on Sephadex LH-20 eluted with a 1:1 MeOH/H<sub>2</sub>O solution to afford 17 fractions. Fractions 15 to 17 (65.8 mg) were combined and separated on a

reversed-phase HPLC column (YMC Pack C8, 5  $\mu$ , 250  $\times$  20 mm, DAD at maximum absorbance, 6:4 H<sub>2</sub>O/CH<sub>3</sub>CN, flow rate 5.0 mL/min) to obtain pure micropeptin SF909 (5.5 mg,  $t_{\text{R}}$  20.0 min, also isolated from cell mass, 16.1 mg, 0.0062% yield based on the dry weight of the cell mass), micropeptin KT1042 (**1**) (4.0 mg,  $t_{\text{R}}$  28.2 min, also isolated from cell mass, 4.8 mg, 0.0025% yield), and the known micropeptin HM978 (5.0 mg,  $t_{\text{R}}$  32.5 min, 0.0014% yield). Combined fractions 9–13 were further separated with fractions from the cell extract. The lyophilized cell mass of IL-347 (350 g) was extracted with 7:3 MeOH/H<sub>2</sub>O (3  $\times$  2 L), and evaporation yielded 28 g of extract. The extract was chromatographed, in 5 g portions, on a reversed-phase (ODS) flash column (YMC-GEL, 120A, 4.4  $\times$  6.4 cm) eluted with an increasing percentage of MeOH in H<sub>2</sub>O. Fraction 3, eluted from the ODS column with 1:4 MeOH/H<sub>2</sub>O (0.5 g), was separated on a Sephadex LH-20 (MeOH/H<sub>2</sub>O, 1:1) column and on a reversed-phase HPLC column (YMC Pack C8, 5  $\mu$ , 250  $\times$  20 mm, DAD at maximum absorbance, 6:4 H<sub>2</sub>O/CH<sub>3</sub>CN, flow rate 5.0 mL/min) to obtain pure microguanidine KT636 (**2**) (5.6 mg, 0.0016% yield). Fractions 4–9 (3:7, 2:3, 1:1, 3:2, and 7:3 MeOH/H<sub>2</sub>O, total of 3.9 g) fully inhibited trypsin and chymotrypsin at a concentration of 1 mg/mL. These fractions were further separated on a Sephadex LH-20 column eluted with 1:1 MeOH/CHCl<sub>3</sub> to obtain 21 fractions. Fractions 10–12 (1.1 g) were combined and separated repeatedly on a reversed-phase HPLC (YMC-Pack C18, 5  $\mu$ , 250  $\times$  20 mm, DAD at maximum absorbance, 7:3 0.1% TFA in H<sub>2</sub>O/CH<sub>3</sub>CN, flow rate 5.0 mL/min) to obtain a semipure fraction (286 mg,  $t_{\text{R}}$  12.9 min) and pure aeruginosin KT650 (**5**) (229.2 mg,  $t_{\text{R}}$  16.9 min, 0.037% yield). The semipure fraction was subjected to the same column and eluted with 55:45 0.1% TFA in H<sub>2</sub>O/MeOH (flow rate 5.0 mL/min) to obtain pure aeruginosin KT608A (**3**) (61.6 mg,  $t_{\text{R}}$  22.6 min, 0.0176% yield), pure aeruginosin KT608B (**4**) (97.0 mg,  $t_{\text{R}}$  29.0 min, 0.0277% yield), and pure pseudoaeruginosin KT554 (2.6 mg,  $t_{\text{R}}$  32.1 min, 0.0007% yield). The known cyanopeptolin S (11.5 mg, 0.0033% yield), planktocylin-S-oxide (5.0 mg, 0.0014% yield), and planktocylin-*iso*-S-oxide (4.5 mg, 0.0013% yield) were isolated from other fractions of the Sephadex LH-20 column. The isolation of aeruginosin GH553 is described elsewhere.<sup>13</sup>

**Micropeptin KT1042 (**1**):** glassy, white solid;  $[\alpha]_{\text{D}}^{23}$  -66 ( $c$  0.41, MeOH); UV (MeOH)  $\lambda_{\text{max}}$  (log  $\epsilon$ ) 203 (4.09), 220 (4.10), 277 (3.50) nm;  $^1\text{H}$  and  $^{13}\text{C}$  NMR (Table 1); HR MALDI-TOF MS  $m/z$  1065.4971 [ $\text{M} + \text{Na}$ ]<sup>+</sup> (calcd for C<sub>53</sub>H<sub>70</sub>N<sub>8</sub>NaO<sub>12</sub>, 1065.4904). Retention times of amino acid Marfey's derivatives: L-Tyr 51.4 min (D-Tyr 53.3 min), L-Thr 33.1 min (D-Thr 35.3 min), L-Glu 34.3 min (D-Glu 35.0 min) L-NMePhe 45.9 min, L-Val 42.0 min (D-Val 44.9 min) L-Gln 32.3 min

(D-Gln 33.0 min). Retention time of amino acid FDAA derivative: L-*allo*-Ile 39.7 min (L-Ile 40.2 min). Retention time of L-hydroxyphenyllactic acid (Hpla) on the chiral-phase column 3.8 min (D-Hpla 4.2 min).

**Microguanidine KT636 (2):** glassy, white solid;  $[\alpha]_D^{23}$  7 (c 0.28, H<sub>2</sub>O); UV (H<sub>2</sub>O)  $\lambda_{\max}$  (log  $\epsilon$ ) 226 (3.61), 277 (3.08) nm; <sup>1</sup>H and <sup>13</sup>C NMR (Table 2); HRESIMS *m/z* 635.1002 [M - H]<sup>-</sup> (calcd for C<sub>19</sub>H<sub>31</sub>N<sub>4</sub>O<sub>14</sub>S<sub>3</sub>, 635.0999).

**Aeruginosin KT608A (3):** glassy, white solid;  $[\alpha]_D^{23}$  -53 (c 0.20, MeOH); UV (MeOH)  $\lambda_{\max}$  (log  $\epsilon$ ) 204 (4.30), 226 (3.90), 278 (3.04) nm; <sup>1</sup>H and <sup>13</sup>C NMR (Tables 3 and S3a); HRESIMS *m/z* 609.3409 [M + H]<sup>+</sup> (calcd for C<sub>32</sub>H<sub>45</sub>N<sub>6</sub>O<sub>6</sub>, 609.3401). Retention times of L-FDAA derivatives of amino acids: D-Phe 48.7 min (L-Phe 46.8 min), D-3a,7a-*diepi*-Choi 31.0 min (L-Choi 38.4 min, L-6-*epi*-Choi, 36.6 min). Retention time of L-Hpla on the chiral-phase column: 3.9 min (D-Hpla 4.2 min).

**Aeruginosin KT608B (4):** glassy white solid;  $[\alpha]_D^{23}$  11 (c 0.23, MeOH); UV (MeOH)  $\lambda_{\max}$  (log  $\epsilon$ ) 204 (4.22), 226 (3.86), 278 (3.00) nm; <sup>1</sup>H and <sup>13</sup>C NMR (Tables 4 and S4a); HRESIMS *m/z* 609.3400 [M + H]<sup>+</sup> (calcd for C<sub>32</sub>H<sub>45</sub>N<sub>6</sub>O<sub>6</sub>, 609.3401). Retention times of L-FDAA derivatives of amino acids: D-Phe 48.7 min (L-Phe 46.8 min), D-3a,7a-*diepi*-Choi 31.0 min (L-Choi 38.4 min, L-6-*epi*-Choi, 36.6 min). Retention time of D-FDAA derivatives of amino acids: L-Phe 48.7 min (D-Phe 46.8 min), D-3a,7a-*diepi*-Choi 29.4 min. Retention time of D-Hpla on the chiral-phase column: 4.2 min (L-Hpla 3.9 min).

**Aeruginosin KT650 (5):** glassy white solid;  $[\alpha]_D^{23}$  -9 (c 0.32, MeOH); UV (MeOH)  $\lambda_{\max}$  (log  $\epsilon$ ) 226 (3.64), 278 (2.84) nm; <sup>1</sup>H and <sup>13</sup>C NMR (Tables 5 and Table S5a); HRESIMS *m/z* 6773.3255 [M + Na]<sup>+</sup> (calcd for C<sub>34</sub>H<sub>46</sub>N<sub>6</sub>NaO<sub>7</sub>, 673.3320). Retention times of L-FDAA derivatives of amino acids: D-Phe 48.7 min (L-Phe 46.8 min), D-3a,7a-*diepi*-Choi 31.0 min (L-Choi 38.4 min, L-6-*epi*-Choi, 36.6 min). Retention time of D-Hpla on the chiral-phase column: 4.2 min (L-Hpla 3.9 min).

**Pseudoaeruginosin KT554 (6):** glassy, white solid;  $[\alpha]_D^{23}$  -36 (c 0.13, MeOH); UV (MeOH)  $\lambda_{\max}$  (log  $\epsilon$ ) 211 (3.41), 230 (3.17) 278 (2.78) nm; <sup>1</sup>H and <sup>13</sup>C NMR (Table 6); HRESIMS *m/z* 555.3280 [M + H]<sup>+</sup> (calcd for C<sub>29</sub>H<sub>43</sub>N<sub>6</sub>O<sub>5</sub>, 555.3295). Retention times of L-FDAA derivatives of amino acids: D-Phe 48.7 min (L-Phe 47.0 min), D-Leu 48.4 min (L-Leu 36.0 min). Retention time of D-Hpla acid on the chiral-phase column: 4.2 min (L-Hpla 3.9 min).

**Aeruginosin GH553 (7):** glassy, white solid;  $[\alpha]_D^{23}$  -88 (c 0.20, MeOH); UV (MeOH)  $\lambda_{\max}$  (log  $\epsilon$ ) 224 (4.04), 278 (3.39) nm; <sup>1</sup>H and <sup>13</sup>C NMR (Tables 7 and S7a); HR MALDI-TOF MS *m/z* 576.2354 [M + Na]<sup>+</sup> (calcd for C<sub>29</sub>H<sub>35</sub>N<sub>3</sub>NaO<sub>8</sub>, 576.2316). Retention times of L-FDAA derivatives of amino acids: D-Tyr 53.0 min (L-Tyr 51.5 min), D-3a,7a-*diepi*-Choi 31.0 min (L-Choi 38.4 min, L-6-*epi*-Choi, 36.6 min). Retention time of L-Hpla on the chiral-phase column: 3.9 min (D-Hpla 4.2 min).

**Micropeptin SF909:** glassy yellow solid;  $[\alpha]_D^{23}$  -33 (c 0.28, MeOH); UV (MeOH)  $\lambda_{\max}$  (log  $\epsilon$ ) 224 (4.10), 278 (3.30) nm; NMR data were found to be identical with reported data;<sup>14</sup> HR MALDI-TOF MS *m/z* 932.4720 [M + Na]<sup>+</sup>.

**Micropeptin HM978:**  $[\alpha]_D^{23}$  -66 (c 0.5, MeOH); UV (MeOH)  $\lambda_{\max}$  (log  $\epsilon$ ) 220 (4.00), 278 (3.30) nm; NMR data were found to be identical with reported data;<sup>12</sup> HR MALDI-TOF MS *m/z* 1001.4955 ([M + Na]<sup>+</sup>).

**Cyanopeptolin S:** glassy, yellow solid;  $[\alpha]_D^{23}$  -28 (c 0.22, MeOH); UV (MeOH)  $\lambda_{\max}$  (log  $\epsilon$ ) 203 (3.96); NMR data were found to be identical with reported data;<sup>15</sup> ESIMS *m/z* 924.4 [M - H]<sup>-</sup>.

**Anabaenopeptin F:** glassy, white solid;  $[\alpha]_D^{23}$  -21 (c 0.55, MeOH); UV (MeOH)  $\lambda_{\max}$  (log  $\epsilon$ ) 215 (4.08), 278 (3.25) nm; NMR data were found to be identical with reported data;<sup>16</sup> HR MALDI-TOF MS *m/z* 851.5114 [M + H]<sup>+</sup>.

**Planktocylin-S-oxide:** glassy, yellow solid;  $[\alpha]_D^{23}$  3.2 (c 0.25, MeOH); UV (MeOH)  $\lambda_{\max}$  (log  $\epsilon$ ) 226 (3.26); NMR data (Table S8a);<sup>17,18</sup> ESIMS *m/z* 839.4 [M + Na]<sup>+</sup>.

**Planktocylin-iso-S-oxide:** glassy, yellow solid;  $[\alpha]_D^{23}$  -3.5 (c 0.23, MeOH); UV (MeOH)  $\lambda_{\max}$  (log  $\epsilon$ ) 226 (3.11); NMR data (Table S8b);<sup>17,18</sup> ESIMS *m/z* 839.4 [M + Na]<sup>+</sup>.

## ■ ASSOCIATED CONTENT

### 📄 Supporting Information

1D and 2D NMR spectra and HRMS data of compounds 1–7, tables of NMR data of the minor rotamers of compounds 3–5 and 7, as well as comparison of the <sup>1</sup>H and <sup>13</sup>C NMR spectra and Marfey's chromatograms of compounds 3 and 4. This material is available free of charge via the Internet at <http://pubs.acs.org>.

## ■ AUTHOR INFORMATION

### Corresponding Author

\*Tel: ++972-3-6408550. Fax: ++972-3-6409293. E-mail: [carmeli@post.tau.ac.il](mailto:carmeli@post.tau.ac.il)

## ■ ACKNOWLEDGMENTS

We thank A. Sacher and K. Shereshevsky, The Mass Spectrometry Laboratory of The Maiman Institute for Proteome Research of Tel Aviv University, for the MALDI mass spectra measurements and N. Tal, the Mass Spectrometry Facility of the School of Chemistry, Tel Aviv University, for the measurements of the HR ESI mass spectra. The authors thank J. Bonjoch, Faculty of Pharmacy, University of Barcelona, Spain, for the kind provision of the synthetic Choi isomers. This research was supported by the Israel Science Foundation grants 037/02 and 776/06.

## ■ REFERENCES

- Burja, A. M.; Banaigs, B.; Abou-Mansour, E.; Burgess, J. G.; Wright, P. C. *Tetrahedron* **2001**, *57*, 9347–9377.
- Tan, L. T. *Phytochemistry* **2007**, *68*, 954–979.
- Wiegand, C.; Pflugmacher, S. *Toxicol. Appl. Pharmacol.* **2005**, *203*, 201–218.
- Gkelis, S.; Harjunpaa, V.; Lanaras, T.; Sivonen, K. *Environ. Toxicol.* **2005**, *20*, 249–256.
- Okino, T.; Murakami, M.; Haraguchi, R.; Munekata, J.; Matsuda, H.; Yamaguchi, K. *Tetrahedron Lett.* **1993**, *34*, 8131–8134.
- Harada, K.; Fujii, K.; Shimada, T.; Suzuki, M.; Sano, H.; Adachi, K.; Carmichael, W. W. *Tetrahedron Lett.* **1995**, *36*, 1511–1514.
- Murakami, M.; Okita, Y.; Matsuda, H.; Okino, T.; Yamaguchi, K. *Tetrahedron Lett.* **1994**, *35*, 3129–3132.
- Ishida, K.; Kato, T.; Murakami, M.; Watanabe, M.; Watanabe, M. F. *Tetrahedron* **2000**, *56*, 8643–8656.
- Reshef, V.; Carmeli, S. *Tetrahedron* **2006**, *62*, 7361–7369.
- Ersmark, K.; Del Valle, J. R.; Hanessian, S. *Angew. Chem., Int. Ed.* **2008**, *47*, 1202–1223.
- Ploutno, A.; Shoshan, M.; Carmeli, S. *J. Nat. Prod.* **2002**, *65*, 973–978.
- Valls, N.; Vallribera, M.; Carmeli, S.; Bonjoch, J. *Org. Lett.* **2003**, *5*, 447–450.
- Lifshits, M.; Zafrir-Ilan, E.; Raveh, A.; Carmeli, S. *Tetrahedron* **2011**, *67*, 4017–4024.
- Banker, R.; Carmeli, S. *Tetrahedron* **1999**, *55*, 10835–10844.
- Jakobi, C.; Oberer, L.; Quiquerez, C.; Konig, W. A.; Weckesser, J. *FEMS Microbiol. Lett.* **1995**, *129*, 129–133.
- Shin, H. J.; Matsuda, H.; Murakami, M.; Yamaguchi, K. *J. Nat. Prod.* **1997**, *60*, 139–141.
- Baumann, H., I.; Keller, S.; Wolter, F., E.; Nicholson, G., J.; Jung, G.; Sussmuth, R., D.; Juttner, F. *J. Nat. Prod.* **2007**, *70*, 1611–1615.
- Pogrobinsky-Grach, O. Ph.D. Thesis, Tel Aviv University, 2009.
- Marfey's reagent: 1-fluoro-2,4-dinitrophenyl-5-L-alanine amide: Marfey, P. *Carlsberg Res. Commun.* **1984**, *49*, 591–596.
- Bowden, K.; Heilbron, I. M.; Jones, E. R. H.; Weedon, B. C. L. *J. Chem. Soc.* **1946**, 39–45.
- Zafrir, E.; Carmeli, S. *J. Nat. Prod.* **2010**, *73*, 352–358.
- Gesner-Apter, S.; Carmeli, S. *Tetrahedron* **2008**, *64*, 6628–6634.

- (23) Wedemeyer, W. J.; Welker, E.; Scheraga, H. A. *Biochemistry* **2002**, *41*, 14637–14644.
- (24) Madi, Z. L.; Griesinger, C.; Ernst, R. R. *J. Am. Chem. Soc.* **1990**, *112*, 2908–2914.
- (25) Fujii, K.; Ikal, Y.; Mayumi, T.; Oka, H.; Suzuki, M.; Harada, K.-I. *Analyt. Chem.* **1997**, *69*, 3346–3352.
- (26) Ishida, K.; Christiansen, G.; Yoshida, W. Y.; Kurmayer, R.; Welker, M.; Valls, N.; Bonjoch, J.; Hertweck, C.; Borner, T.; Hemscheidt, T.; Dittmann, E. *Chem. Biol.* **2007**, *14*, 565–576.